AD-A063 187 FOREIGN TECHNOLOGY DIV WRIGHT-PATTERSON AFB OHIO F/G 4/2
THE APPLICATIONS OF FINITE-ELEMENT METHOD IN NUMERICAL WEATHER --ETC(U)
FEB 78 S C SZE, C S CHIEH
UNCLASSIFIED FTD-ID(RS)T-2338-77 NL

1 OF 1
AD A
063187

END
DATE
FILMED
3 -79
DDC

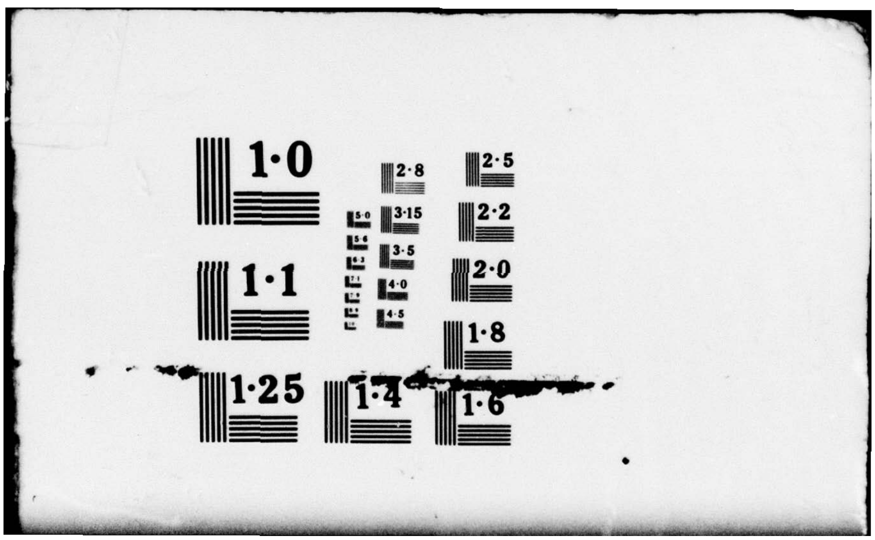
1·0
2·8
2·5
5·0
3·15
2·2
5·6
3·5
2·0
1·1
4·0
4·5
1·8
1·25
1·4
1·6

FTD-ID(RS)T-2338-77

AD-A063187

FOREIGN TECHNOLOGY DIVISION

(1)

AIR FORCE SYSTEMS COMMAND

THE APPLICATIONS OF FINITE-ELEMENT METHOD IN NUMERICAL WEATHER FORECAST

by

Shen Chang Sze, Chen Shih Chieh

FOREIGN TECHNOLOGY DIVISION

Approved for public release; distribution unlimited.

78 12 22 356

EDITED TRANSLATION

FTD-ID(RS)T-2338-77 27 February 1978

MICROFICHE NR: FTD-78-C-000288

THE APPLICATIONS OF FINITE-ELEMENT METHOD IN NUMERICAL WEATHER FORECAST

By: Shen Chang Sze, Chen Shih Chieh

English pages: 11

Source: Kexue Tongbao, Vol. 22, No. 6, 1977, Peking, pp. 263-266.

Country of origin: China
Translated by: SCITRAN
F33657-76-D-0390
Requester: FTD/WE

PREPARED BY:

TRANSLATION DIVISION
FOREIGN TECHNOLOGY DIVISION
WP-AFB, OHIO.

THE APPLICATIONS OF FINITE-ELEMENT METHOD IN NUMERICAL WEATHER FORECAST

Mathematics Department
Shantung University

and

Shen Chång Sze and Chen Shih Chieh
Weather Bureau, Shantung Province

(received December 15, 1975)

The finite-element method has wide applications in structural mechanics and elasticity mechanics.[1,2] In the last two or three years, the possibility of applying finite-element methods to numerical weather forecast has been investigated from a theoretical point of view.[3,4] This article is a discussion of such applications based on a positive-pressure vorticity equation. The grid division used consists of large and small rectangles. Such grids have manifested effectiveness in improving the forecast accuracy of the region under consideration, and they are also economical in terms of computer storage. Although rectangular grids are employed in some foreign nations, the finite-difference method is always used in the computation. In the finite-difference method, calculations are performed twice (or three times), namely, calculations are done first on the coarse grid and then on the fine division grids locally. In so doing, artificial boundary conditions must be imposed on the boundaries of the local fine grids. Such difficulties can be overcome by the finite-element method. Judging from the calculations for the situations studied, the application of the finite-element method in numerical weather forecast is a meaningful undertaking from both practical and theoretical standpoints. It should be pointed out that the finite-element method allows one to generalize the Arakawa scheme[5], a scheme usually used in overcoming the nonlinear instability, to the general grid division and obtain a neat and rigorous proof of the conservation laws. Since the energy conservation problem for an arbitrary grid is solved, it would be eventually possible to carry out numerical forecast using monitor station values directly.

In the course of our numerical calculation, Jespersen's work[6] came to our attention. He also discovered that the Arakawa scheme is an inevitable result of the finite-element method. However, Jespersen considered only the situation of equal distance grids. Hence, Jespersen's work is a special case of our development.

I. Finite-Element Equation *

For the sake of simplicity, consider the initial boundary value problem of a positive pressure vorticity equation.

$$-\Delta\left(\frac{\partial\Phi}{\partial t}\right) + \frac{\mu^2}{m^2}\frac{\partial\Phi}{\partial t} = J\left(\Phi, \frac{m^2}{f}\Delta\Phi + f\right),\ (x,y)\in G, \quad \text{---} (1)$$

$$\left.\frac{\partial\Phi}{\partial t}\right|_{\partial G} = 0 \quad \text{-----} (2) \qquad \Phi\Big|_{t=0} = \Phi^0 \quad \text{-----} (3)$$

The notations employed here are the ones commonly used in numerical weather forecast. G is the rectangular forecast region and ∂G is the boundary of G.

This article was received on the 5th of December 1975.

*Computational mathematics major grade 72 students of the Mathematics Department, Shantung University, participated in numerical calculations. Comrade Chang Ching Hua of the Shantung Province Weather Bureau participated in some data reduction and graphing.

In order to arrive at the finite-element equations of (1) and (2), they are transformed to their equivalent variation problems (1), (2). That is, among the proper smooth functions satisfying the boundary condition $u|_{\partial G} = 0$, the general function F (u) given below is minimized to the function $u(x, y)$, where $u = \partial\Phi/\partial t$.

$$F(u) = \iint_G \left\{ \left(\frac{\partial u}{\partial x}\right)^2 + \left(\frac{\partial u}{\partial y}\right)^2 + \frac{\mu^2}{m^2} u^2 - 2uJ\left(\Phi, \frac{m^2}{f}\Delta\Phi + f\right) \right\} dx\,dy \qquad (4)$$

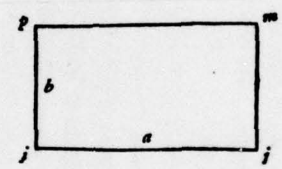

Fig. 1

According to the finite-element method, region G is divided into a number of rectangular elements. We assume u to be continuous on G and to be a bilinear function of each rectangle. The apices of the rectangular element $\square_e$ are i, j, m, and p, and the lengths of the two sides are a and b (see Fig. 1). The coordinates of points i, j, m and p are (x_i, y_i), (x_j, y_j), (x_m, y_m), and (x_p, y_p) respectively. The transformation

$$\begin{aligned} x &= x_i + a\xi, \\ y &= y_i + b\eta, \end{aligned} \qquad (5)$$

changes the unit rectangle to a unit square in the (ξ , η) plane with (0, 0) and (1, 1) being its diagonal apices. The bilinear interpolation function on this element $\square_e$ can then be shown to be

$$\begin{aligned} u(x, y) &= (1 - \xi - \eta + \xi\eta)u_i \\ &+ (\xi - \xi\eta)u_j + \xi\eta u_m + (\eta - \xi\eta)u_p, \end{aligned} \qquad (6)$$

where U_i, U_j, U_m and U_p are the values of $U(x, y)$ at node points i, j, m, and p, respectively. On $\square_e$, let

$$\zeta = \frac{m^2}{f} \Delta \Phi + f, \tag{7}$$

functions Φ and ζ can also be expressed in terms of bilinear interpolation function similar to (6):

$$\begin{aligned} \Phi(x,y) &= (1-\xi-\eta+\xi\eta)\Phi_i + (\xi-\xi\eta)\Phi_j + \xi\eta\Phi_m + (\eta-\xi\eta)\Phi_p, \\ \zeta(x,y) &= (1-\xi-\eta+\xi\eta)\zeta_i + (\xi-\xi\eta)\zeta_j + \xi\eta\zeta_m + (\eta-\xi\eta)\zeta_p, \end{aligned} \tag{8}$$

here subscipted quantities are values of the respective functions at points indicated by the subscripts. One can then write down:

$$\begin{aligned} J(\Phi,\zeta) &= \frac{\partial\Phi}{\partial x}\frac{\partial\zeta}{\partial y} - \frac{\partial\Phi}{\partial y}\frac{\partial\zeta}{\partial x} \\ &= \frac{1}{ab}\big[(1-\eta)(\Phi_i\zeta_j - \Phi_j\zeta_i) + (\eta-\xi)(\Phi_i\zeta_m - \Phi_m\zeta_i) \\ &\quad + \xi(\Phi_j\zeta_m - \Phi_m\zeta_j) + \eta(\Phi_m\zeta_p - \Phi_p\zeta_m) \\ &\quad + (1-\eta-\xi)(\Phi_j\zeta_p - \Phi_p\zeta_j) + (\xi-1)(\Phi_i\zeta_p - \Phi_p\zeta_i)\big] \end{aligned} \tag{9}$$

The set of algebraic equations satisfied by the values of U at the nodes can be obtained by substituting (6) and (9) into (4), evaluating the integral, and then, according to variation principles, finding the minima of all U_k. This set of equations is commonly known as the finite-element equation.

Fig. 2

If point 0 is an inner node, the only relevant values of u in finding the equations with respect to point 0 using the method described above are those at the nine corners of the four adjacent rectangles sharing point 0 as their common apex. If the nodes are indexed as shown in Fig. 2, the finite-element equation obtained with respect to point 0 is:

$$\sum_{i=0}^{8} K[i]u_i = b[0], \tag{10}$$

where the coefficients are listed below:

$$\left\{\begin{aligned}
K[0] &= \frac{b_1}{3a_1} + \frac{a_1}{3b_1} + \frac{b_1}{3a_2} + \frac{a_2}{3b_1} \\
&\quad + \frac{b_2}{3a_2} + \frac{a_2}{3b_2} + \frac{b_2}{3a_1} + \frac{a_1}{3b_2} \\
&\quad + \frac{1}{9}(T_1 + T_2 + T_3 + T_4), \\
K[1] &= -\frac{b_1}{3a_1} + \frac{a_1}{6b_1} - \frac{b_2}{3a_1} + \frac{a_1}{6b_2} \\
&\quad + \frac{1}{18}(T_4 + T_1), \\
K[2] &= \frac{b_1}{6a_1} - \frac{a_1}{3b_1} + \frac{b_1}{6a_2} - \frac{a_2}{3b_1} \\
&\quad + \frac{1}{18}(T_1 + T_2), \\
K[3] &= -\frac{b_1}{3a_2} + \frac{a_2}{6b_1} - \frac{b_2}{3a_2} + \frac{a_2}{6b_2} \\
&\quad + \frac{1}{18}(T_2 + T_3), \\
K[4] &= \frac{b_2}{6a_2} - \frac{a_2}{3b_2} + \frac{b_2}{6a_1} - \frac{a_1}{3b_2} \\
&\quad + \frac{1}{18}(T_3 + T_4), \\
K[5] &= -\frac{b_1}{6a_1} - \frac{a_1}{6b_1} + \frac{T_1}{36}, \\
K[6] &= -\frac{b_1}{6a_2} - \frac{a_2}{6b_1} + \frac{T_2}{36}, \\
K[7] &= -\frac{b_2}{6a_2} - \frac{a_2}{6b_2} + \frac{T_3}{36}, \\
K[8] &= -\frac{b_2}{6a_1} - \frac{a_1}{6b_2} + \frac{T_4}{36},
\end{aligned}\right. \tag{11}$$

$$T_1 = \frac{\mu^2}{m^2} a_1 b_1, \; T_2 = \frac{\mu^2}{m^2} a_2 b_1,$$

$$T_3 = \frac{\mu^2}{m^2} a_2 b_2, \; T_4 = \frac{\mu^2}{m^2} a_1 b_2.$$

The right hand side term of Eq. (10) is

$$b[0] = \frac{1}{12}\left(G_0^{++} + G_0^{+x} + G_0^{x+} \right), \qquad (12)$$

where

$$\left\{ \begin{aligned} G_0^{++} &= (\Phi_1 - \Phi_3)(\zeta_2 - \zeta_4) - (\Phi_2 - \Phi_4)(\zeta_1 - \zeta_3) \\ G_0^{+x} &= \Phi_1(\zeta_5 - \zeta_8) - \Phi_3(\zeta_6 - \zeta_7) - \Phi_2(\zeta_5 - \zeta_6) + \Phi_4(\zeta_8 - \zeta_7) \\ G_0^{x+} &= \zeta_2(\Phi_5 - \Phi_6) - \zeta_4(\Phi_8 - \Phi_7) - \zeta_1(\Phi_5 - \Phi_8) + \zeta_3(\Phi_6 - \Phi_7) \end{aligned} \right. \qquad (13)$$

If Eq. (10) is multiplied by $4/[(a_1 + a_2)(b_1 + b_2)]$, it can easily be seen that, when grids are equal distant ($a_1 = a_2 = b_1 = b_2 = h$), the above equation is similar to the Helmholz equation with an average nine-point difference scheme; furthermore, the right hand side term is exactly the Arakawa conservation expression.(5)

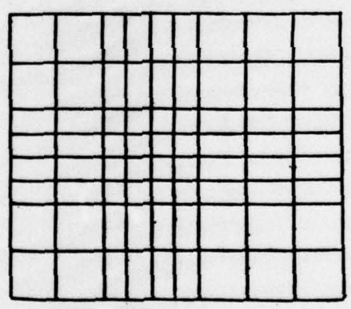

Fig. 3 Large grid distance is h and small grid distance is h/2. (h = 540 km)

We divide the forecast region G into grids of intervals h and h/2 (h is 540 km) as shown in Fig. 3. The finite-element equation obtained with the method described above is then solved to get the values of the function $u = \partial\Phi/\partial t$ at grid nodes. The conventional three-step method is then used to extrapolate the forecast field Φ at 24 and 48 hours with a time interval Δt of ½ hour. In calculating the term on the right hand side, the values of $\Delta\Phi$ at the nodes are arrived at by Spline extrapolation and the values of ζ at the nodes are then obtained.** The results of our numerical computation indicated that the grids are stable and that no spatial smoothing was necessary during the computation. The resultant 48 hour forecast diagram was relatively close to the true situation. Contrary to the finite difference method where additional boundary conditions are imposed, the finite-element method gives rise to the equations at the boundary nodes.

II. Generalization of the Arakawa Conservation and Energy Conservation

Definition:

$$J_0 = \frac{\sum_{e'} \iint_{\square_{e'}} J(\Phi, \zeta) N_{e'}\, dx\, dy}{\sum_{e'} \iint_{\square_{e'}} N_{e'}\, dx\, dy}, \tag{14}$$

where $\square_{e'}$ is any element containing point 0 as an apex and the summation is over all such elements. The factor $N_{e'}$ has the following convention: If $\square_{e'}$ is a rectangle and point 0 assumes the "i" corner of $\square_{e'}$, then $N_{e'} = N_1 = (1 - \xi - \eta + \xi\eta)$; when point 0 assumes the "j" corner in element $\square_{e'}$, $N_{e'} = N_2 = (\xi - \xi\eta)$; when point 0 is the "m" corner of $\square_{e'}$, $N_{e'} = N_3 = \xi\eta$, and finally when point 0 is the "p" corner of $\square_{e'}$, $N_{e'} = N_4 = \eta - \xi\eta$.

** The value of ζ at the nodes can be obtained by the following equation if Spline extrapolation value is not used:

$$(\Delta\Phi)_0 = 4 \sum_{i=0}^{8} K[i]\, \Phi_i \,/\, [(a_1 + a_2)(b_1 + b_2)],$$

A similar equation can be derived for the boundary points.

Eq. (14) is the dispersion formula of $J(\Phi, \zeta)$. The denominator of Eq. (14) as S_0. If point 0 is the inner node shown in Fig. 2, Eq. (14) gives

$$J_0 = \frac{G_0^{++} + G_0^{+\times} + G_0^{\times +}}{3(a_1 + a_2)(b_1 + b_2)}, \tag{15}$$

where G_0^{++}, G_0^{+x} and G_0^{x+} are given in Eq. (13). When $S_0 = 4/[(a_1 + a_2)(b_1 + b_2)]$, Eq. (15) reduces to $b[o] / S_0$. Thus, expression (15) is consistent with the right hand term of Eq. (10), which is Eq. (12) divided by S_0 and, obviously, it is the generalization of Arakawa's conservation. When $a_1 = a_2 = b_1 = b_2 = h$, Eq. (15) becomes the usual Arakawa conservation expression:

$$J_0 = \frac{1}{3}(J_0^{++} + J_0^{+\times} + J_0^{\times +}),$$

where $J_0^{++} = \frac{1}{4h^2} G_0^{++}$, $J_0^{+\times} = \frac{1}{4h^2} G_0^{+\times}$, $J_0^{\times +} = \frac{1}{4h^2} G_0^{\times +}$. Eq. (15) is the generalized Arakawa conservation for nonuniform rectangular grids and Eq. (14) is the generalized Arakawa conservation for an arbitrary grid.

Eq. (14) also satisfied the following three conservation relations:

$$\sum_0 J_0 S_0 = 0 \text{ (Conservation of mean vorticity)} \tag{16}$$

$$\sum_0 \Phi_0 J_0 S_0 = 0 \text{ (Conservation of mean kinetic energy)} \tag{17}$$

$$\sum_0 \zeta_0 J_0 S_0 = 0 \text{ (Conservation of mean square vorticity)} \tag{18}$$

where 0 assumes all nodes including nodes on the boundary and S_0 is the denominator of Eq. (14).

As a matter of fact, since Jocobian satisfies the conservation of mean vorticity:

$$\iint_G J(\Phi, \zeta)\, dxdy = 0,$$

we have

$$\sum_e \iint_{\square_e} J(\Phi, \zeta)\, dxdy = 0. \tag{19}$$

Notice that $\sum_{i=1}^{4} N_i = 1$,

hence,

$$\iint_{\square_e} J(\Phi, \zeta)\, dxdy = \sum_{i=1}^{4} \iint_{\square_e} J(\Phi, \zeta)\, N_i\, dxdy. \tag{20}$$

From Eq. (14), we have

$$\sum_0 J_0 S_0 = \sum_0 \sum_{e'} \iint_{\square_{e'}} J(\Phi, \zeta)\, N_{e'}\, dxdy,$$

and the above expression can be rewritten by changing the summation over nodes 0 to a summation over all elements $\square_e$:

$$\sum_0 J_0 S_0 = \sum_e \sum_{i=1}^{4} \iint_{\square_e} J(\Phi, \zeta)\, N_i\, dxdy,$$

and from (19) and (20), we have

$$\sum_0 J_0 S_0 = 0 \text{ (Conservation of mean vorticity).}$$

The proof of (17) and (18) are the same so only the proof of (17) will be given below. From the integral form expression of the conservation of mean kinetic energy, we have

$$\iint_G \Phi J(\Phi, \zeta)\, dxdy = \sum_e \iint_{\square_e} \Phi J(\Phi, \zeta)\, dxdy = 0. \tag{21}$$

Further, from (14) we have

$$\sum_0 \Phi_0 J_0 S_0 = \sum_0 \Phi_0 \sum_{e'} \iint_{\square_{e'}} J(\Phi, \zeta) N_{e'}\, dx dy$$

$$= \sum_0 \sum_{e'} \iint_{\square_{e'}} \Phi_0 J(\Phi, \zeta) N_{e'}\, dx dy,$$

where $\sum_{e'}$ is the summation over all rectangles $\square_{e'}$ having point 0 as an apex. Again change the summation over nodes to a summation over each element $\square_e$, it can be seen that the equation above becomes:

$$\sum_0 \Phi_0 J_0 S_0 = \sum_e \sum_{i=1}^{4} \iint_{\square_e} \Phi_{ei}\, J(\Phi, \zeta) N_i\, dx dy, \tag{22}$$

where Φ_{ei} (i = 1, 2, 3, 4) represents the value of Φ at the four corners i, j, m, and p of the element $\square_e$: $\Phi_{e_1} = \Phi_i$, $\Phi_{e_2} = \Phi_j$, $\Phi_{e_3} = \Phi_m$ and $\Phi_{e_4} = \Phi_p$. From the bilinear interpolation equation (8), it is evident that on the element $\square_e$, we have:

$$\sum_{i=1}^{4} \Phi_{ei} N_i = \Phi_i N_1 + \Phi_j N_2 + \Phi_m N_3 + \Phi_p N_4 = \Phi$$

Substituting the above expression into (22) and using Eq. (21), we obtain

$$\sum_0 \Phi_0 J_0 S_0 = \sum_e \iint_{\square_e} \Phi\, J(\Phi, \zeta)\, dxdy = 0$$

and thus completed the proof of (17). Eq. (18) can be proven in a similar manner.

In conclusion, the J_0 defined in Eq. (14) satisfies relations (16) through (18). Generalization of this kind cannot be achieved by the difference method; furthermore, the proof of the three conservation relationships using the finite-element method is simpler and more rigorous as compared to the proof of Arakawa even for the case of equal distance grids where conservations can be proven by the difference method.

References:

1. Feng K'ang, The Practice and Knowledge of Mathematics, 1974, 4; 1975, 1 - 2.
2. Chikiwitz, Finite - Element Methods in Structural and Continuum Mechanics, Defense Industry Publication, 1973.
3. Cullen, M.J.P., J. Inst. Maths. Applics, 11 (1973), 15 - 31.
4. Cullen, M.J.P., J. Inst. Maths. Applics, 13 (1974), 233 - 247.
5. Arakawa, A., J. Computational Phys., 1 (1966), 119 - 143.
6. Jespersen, D.C., J. Computational Phys., 16 (1974), 383 - 390.

DISTRIBUTION LIST

DISTRIBUTION DIRECT TO RECIPIENT

ORGANIZATION		MICROFICHE
A205	DMATC	1
A210	DMAAC	2
B344	DIA/RDS-3C	8
C043	USAMIIA	1
C509	BALLISTIC RES LABS	1
C510	AIR MOBILITY R&D LAB/FIO	1
C513	PICATINNY ARSENAL	1
C535	AVIATION SYS COMD	1
C591	FSTC	5
C619	MIA REDSTONE	1
D008	NISC	1
H300	USAICE (USAREUR)	1
P005	ERDA	1
P055	CIA/CRS/ADD/SD	1
NAVORDSTA (50L)		1
NASA/KSI		1
AFIT/LD		1

ORGANIZATION		MICROFICHE
E053	AF/INAKA	1
E017	AF/ RDXTR-W	1
E404	AEDC	1
E408	AFWL	1
E410	ADTC	1
E413	ESD	2
	FTD	
	CCN	1
	ETID	3
	NIA/PHS	1
	NICD	5